Experimental Neurology 283 (2016) 264–275

Contents lists available at ScienceDirect

Experimental Neurology

journal homepage: www.elsevier.com/locate/yexnr

Research Paper

Endogenous hypothermic response to hypoxia reduces brain injury: Implications for modeling hypoxic-ischemic encephalopathy and therapeutic hypothermia in neonatal mice

Barbara S. Reinboth, Christian Köster, Hanna Abberger, Sebastian Prager, Ivo Bendix, Ursula Felderhoff-Müser, Josephine Herz *

Department of Pediatrics I/Neonatology, University Hospital Essen, University Duisburg-Essen, Essen, Germany

ARTICLE INFO

Article history:
Received 4 March 2016
Received in revised form 15 June 2016
Accepted 22 June 2016
Available online 25 June 2016

Keywords:
Hypoxia-ischemia
Perinatal asphyxia
Therapeutic hypothermia
Neonatal mice
Endogenous temperature regulation
Brain injury
Functional deficits

ABSTRACT

Hypothermia treatment (HT) is the only formally endorsed treatment recommended for hypoxic-ischemic encephalopathy (HIE). However, its success in protecting against brain injury is limited with a number to treat of 7–8. The identification of the target mechanisms of HIE in combination with HT will help to explain ineffective therapy outcomes but also requires stable experimental models in order to establish further neuroprotective therapies. Despite clinical and experimental indications for an endogenous thermoregulatory response to HIE, the potential effects on HIE-induced brain injury have largely been neglected in pre-clinical studies. In the present study we analyzed gray and white matter injury and neurobehavioral outcome in neonatal mice considering the endogenous thermoregulatory response during HIE combined with HT. HIE was induced in postnatal day (PND) 9 C57BL/6 mice through occlusion of the right common carotid artery followed by one hour of hypoxia. Hypoxia was performed at 8% or 10% oxygen (O_2) at two different temperatures based on the nesting body core temperature. Using the model which mimics the clinical situation most closely, i.e. through maintenance of the nesting temperature during hypoxia we compared two mild HT protocols (rectal temperature difference 3 °C for 4 h), initiated either immediately after HIE or with delay of 2 h. Injury was determined by histology, immunohistochemistry and western blot analyses at PND 16 and PND 51. Functional outcome was evaluated by Rota Rod, Elevated Plus Maze, Open Field and Novel Object Recognition testing at PND 30–PND 36 and PND 44–PND 50. We show that HIE modeling in neonatal mice is associated with a significant endogenous drop in body core temperature by 2 °C resulting in profound neuroprotection, expressed by reduced neuropathological injury scores, reduced loss of neurons, axonal structures, myelin and decreased astrogliosis. Immediately applied post-hypoxic HT revealed slight advantages over a delayed onset of therapy on short- and long-term histological outcome demonstrated by reduced neuropathological injury scores and preservation of hippocampal structures. However, depending on the brain region analyzed neuroprotective effects were similar or even reduced compared to protection by endogenous cooling during HIE modeling. Moreover, long-term neurobehavioral outcome was only partially improved for motoric function (i.e. Rota Rod performance and rearing activity) while cognitive deficits (i.e. novel object recognition) remained unchanged. These findings emphasize the need to maintain the nesting temperature during the initiation of the pathological insult and highlight the urgency to develop and assess new adjuvant therapies for HT in well-defined experimental models.

1. Introduction

Perinatal asphyxia may cause hypoxic-ischemic encephalopathy (HIE), which is a significant contributor to neonatal mortality and often leads to long-lasting neurological deficits in neonates. To date, the only officially recommended therapeutic intervention is a hypothermia treatment (HT), (ILCOR guidelines 2015). However, 40–50% of cooled infants still suffer from neurological problems because it is only effective in mild or moderate HIE with a number to treat of 7–8 to prevent one child from dying or having neurodevelopmental disability (Azzopardi et al., 2014; Jacobs et al., 2013). Therefore, current research focuses on the development of adjuvant therapies revealing promising effects in rodent and large animal models (Hobbs et al., 2008; Liu et al., 2004; Ma et al., 2005; Robertson et al., 2013). Nevertheless,

* Corresponding author at: Department of Pediatrics I/Neonatology, University Hospital Essen, University Duisburg-Essen, Hufelandstr. 55, 45147 Essen, Germany.
E-mail address: josephine.herz@uk-essen.de (J. Herz).

http://dx.doi.org/10.1016/j.expneurol.2016.06.024

experimental models of HIE and therapeutic hypothermia are not standardized which may explain some of the contradicting results of its therapeutic efficacy comparing experimental and clinical studies.

The most commonly used pre-clinical model for HIE is the Rice-Vannucci model in postnatal day 7 rats (Rice et al., 1981) which has also been adapted to mice (Ditelberg et al., 1996; Sheldon et al., 1998). Whereas a huge body of evidence suggests protective effects of hypothermia in neonatal rats (Bona et al., 1998; Dalen et al., 2012; Hobbs et al., 2008; Ma et al., 2005; Sabir et al., 2012; Thoresen et al., 1996; Wagner et al., 2002) only few studies were conducted in neonatal term-equivalent mice with inconsistent results regarding short- and long-term protection (Burnsed et al., 2015; Carlsson et al., 2012; Griesmaier et al., 2014; Lin et al., 2014; Zhu et al., 2006). As such, moderate HT for 4 to 5 h started immediately after the insult in neonatal mice has been shown either to provide only short-term protection from brain tissue loss (Burnsed et al., 2015) or to protect only specific regions (Carlsson et al., 2012). Contradicting results have also been observed regarding the onset of therapy. A 6-h delay of 90 min HT at 33 °C was described to confer protection in PND 7 rats at 1 week after the insult (Ma et al., 2005). In contrast the study by Sabir et al. suggests that HT provides protection only when initiated immediately or 3 h post HIE but not with a delay of 6 h (Sabir et al., 2012). One major limitation probably accounting for limited efficacy and inconsistent results might be insufficient monitoring and control of individual body core temperatures under physiological conditions but also during HIE and HT modeling. This is of particular interest since clinical observations imply a compensatory down-regulation of body temperature after HIE which have, however, found little attention in pre-clinical studies and might explain difficulties in translation (Jayasinghe, 2015; Robertson et al., 2008).

Considering the potential impact of endogenous thermoregulation and of exogenously applied hypothermia on the development of HIE-induced brain injury we addressed two major questions with potential impact on both, critical care in humans but also on experimental modeling. First, we investigated whether HIE is associated with endogenous thermoregulatory responses of neonatal mice and whether these correlate with the development of gray and white matter injury. Second, maintaining temperatures at the physiological level of healthy uninjured subjects during HIE, we directly compared two clinically relevant therapeutic hypothermia protocols and their effect on brain damage and neurodevelopmental outcome.

2. Materials and methods

2.1. Modeling hypoxia-ischemia and therapeutic hypothermia in neonatal mice and group allocation

Experiments were performed in accordance to the ARRIVE guidelines and the National Institutes of Health (NIH) Guidelines for the Care and Use of Laboratory Animals with local government approval by the State Agency for Nature, Environment and Consumer Protection North Rhine-Westphalia. Based on the Rice-Vannucci model (Rice et al., 1981) modified for neonatal mice (Ditelberg et al., 1996; Sheldon et al., 1998) hypoxic-ischemic encephalopathy (HIE) was induced in postnatal day (PND) 9 C57BL/6 mice (4.77 ± 0.34 g) through cauterization (high temperature cauter, 1200 °C, Bovie, USA) of the right common carotid artery (CCA) under isoflurane anesthesia (1.5–4 vol%, total duration of surgery: 5–7 min) followed by one hour hypoxia after one hour recovery with their dams. Hypoxia was performed in an air-tight oxygen chamber (OxyCycler, Biospherix, USA) at 8% or 10% oxygen (O_2, remaining nitrogen). Constant body core temperature was maintained through a warming mat (Harvard Apparatus, USA) set to mat surface temperatures of 31 °C (exact temperature: 30.9 ± 0.1 °C, measured with a digital infrared thermometer, Proscan, Dostman GmbH, Germany) or 32 °C (exact temperature: 31.8 ± 0.1 °C). Body temperature was measured with a rectal probe for neonatal mice (RET-4, Physitemp Instruments INC, USA) connected to a digital thermometer (TH-5, Physitemp Instruments INC, USA). Sham-operated animals received anesthesia and neck incision only. Hypothermia (HT) treatment was applied either immediately or 2 h after HIE for the duration of 4 h. Therefore, mice were placed on a custom-made hypothermia plate with temperature control by water circulation resulting in a plate surface temperature of 27 °C (exact temperature: 27.3 ± 0.1 °C). The selected treatment protocols are based on the first pre-clinical hypothermia trial in neonatal mice (Carlsson et al., 2012). The target temperature of 32 °C was achieved within 10 min. Control mice (normothermia, NT) were placed on a warming mat to maintain physiological body core temperatures. Animals per litter and experiment were randomly assigned to the operator by an independent scientist not involved in data acquisition. On the basis of delivery each litter was given a number and each animal was given a permanent additional number. To control the potential influence of weight and sex a stratified randomization was performed. After all pups were assigned to blocks (e.g. sex), simple randomization was performed within each block to assign pups to individual treatment groups. Individuals involved in data analysis knew the animals' permanent designation but were blinded to group assignment.

A total of 286 (137 female, 149 male) mice were enrolled in the study. The first set of mice ($n = 54$; 24 female, 30 male) was used to compare brain injury at PND 16 in two models of HIE differing in ambient temperatures and hypoxic severity during hypoxia. The second cohort of mice ($n = 36$; 17 female, 19 male) was used to evaluate short-term effects of two models of post-hypoxic HT on brain injury at PND 16. In the third set of mice ($n = 81$; 38 female, 43 male) long- term effects of HT on functional and histological outcome were determined. For all animals rectal temperatures were determined at the same frequency (i.e. nesting = immediately when pups were taken from the dam, before and after hypoxia, before and after HT/NT). An additional set of mice was used to measure rectal temperatures (I) at 30, 60 and 180 min after onset of HT/NT (sham: $n = 10$, normothermia: $n = 14$, hypothermia: $n = 14$), (II) after 60 min of normoxia (21% O_2) or hypoxia (8% O_2) at a warming mat set to 31 °C surface temperature (naïve after normoxia: $n = 15$, CCA-occlusion after normoxia: $n = 12$, sham after normoxia: $n = 10$, sham after hypoxia: $n = 10$) and (III) after 60 min of normoxia (21% O_2) at a warming mat set to 32 °C surface temperature (sham: $n = 10$, naïve: $n = 10$, CCA-occlusion: $n = 10$). These mice were not included in tissue analysis. A detailed scheme listing diagrams of all experiments preformed including group allocation and mortality rates are provided in Supplementary Fig. 1 and Table 1.

2.2. Analysis of tissue injury and immunohistochemistry

For assessment of brain tissue atrophy and immunohistochemical analyses, mice were deeply anesthetized with Chloralhydrate (200 mg/kg body weight) and transcardially perfused with ice-cold phosphate buffered saline (PBS). Brains were removed and snap frozen on dry ice. To determine tissue injury and brain tissue loss, 20 μm cryostat sections were stained with cresyl violet. At PND 16 brain injury was assessed according to previously described neuropathological scoring systems (Schlager et al., 2011; Sheldon et al., 1998). Briefly, 8 regions were scored: the anterior, middle and posterior cortex, CA1, CA2, CA3 and dentate gyrus of the hippocampus, and the striatum. Each region was given a rating from 0 to 3 (0- no detectable cell loss, 1- small focal areas of neuronal cell loss, 2- columnar damage in the cortex or moderate to severe cell loss in the other regions, 3- cystic infarction and gliosis). The sum score from different regions was calculated for each animal resulting in a total maximum score of 24. Brain atrophy was determined by measurement of intact areas in ipsilateral and contra-lateral hemispheres at a distance of 400 μm using Image J software (NIH, USA). Volumes were calculated for the total hemisphere and cortex between +1 mm and −2.6 mm from bregma, for the striatum between +1 mm and −0.6 mm from bregma and for the hippocampus between −0.6 mm and −2.6 mm from bregma. Tissue loss was determined by

comparison with contralateral volumes according to the following equation: 1- (volume ratio (left vs right)) × 100.

For assessment of neuronal and oligodendrocyte density cryostat sections taken at the level of +0.2 mm to +0.3 mm from bregma (striatal level) and −1.9 mm to −2.0 mm from bregma (hippocampal level) were used for immunohistochemical detection of NeuN and Olig2. Briefly, sections were thawed and dried at 37 °C followed by fixation in ice-cold 4% PFA for 10 min at 4 °C and blocking with 1% BSA, 0.3% cold fish skin gelatin (Sigma Aldrich, Germany), 0.05% Tween 20 in Tris-buffered saline (TBS) for 1 h at room temperature. Sections were incubated with the following primary antibodies: rabbit anti mouse Olig2, 1:100 (Millipore, Germany); rabbit anti mouse NeuN, 1:500 (Millipore, USA), rabbit anti human Ki67 (1:100, abcam, UK), mouse *anti*-mouse NeuN (1:100, Millipore), mouse anti mouse Olig2 (1:100, Millipore), anti mouse GFAP (1:500, Invitrogen, USA) in blocking solution at 4 °C overnight. Antibody binding was visualized by incubation with the appropriate secondary antibodies (anti-rabbit Alexa Fluor 488 or anti-mouse Alexa Fluor 594, both 1:500, Invitrogen, Germany) for 1 h at room temperature. Nuclei were counterstained with 4′,6-Diamidin-2-phenylindol (Dapi, 100 ng/ml; Molecular Probes, USA). Defined non-overlapping regions of interest (ROI, each 61,220 μm^2) were visualized by fluorescence microscopy (40× objective; Axioplan; Zeiss, Germany) connected to a CCD camera (Microfire; AVT Horn, Germany). At the level of the striatum 6 defined ROIs were analyzed in each hemisphere (3 ROIs in the cortex and 3 ROIs in the striatum). At the level of the hippocampus 6 ROIs (3 ROIs in the cortex and 3 ROIs (CA1, CA2, CA3) in the hippocampus) were evaluated in each hemisphere. Olig2$^+$ DAPI$^+$ cells were counted as oligodendrocytes. For the assessment of neuronal loss and astrogliosis, the neuronal and astrocyte density was quantified by determining the NeuN and GFAP positive area because single cell counting in dense packed regions (e.g. hippocampus (NeuN) and striatum (GFAP)) could not be applied.

2.3. Western Blotting

For western blot analysis ipsi- and contralateral parts of 8 × 20 μm tissue sections within the range of 0.5 mm to 0 mm from bregma (striatal level) and −1.9 mm to −2.3 mm from bregma (hippocampal level) were scratched from object slides and homogenized in ice-cold lysis buffer (RIPA, Sigma-Aldrich) containing protease and phosphatase inhibitors (cOmplete, Roche) and 100 mM PMSF (Sigma-Aldrich). Samples were centrifuged at 4 °C for 20 min (17,000 ×*g*) and the supernatant was collected followed by determination of the protein concentration using the Pierce BCA- protein assay kit (Thermo Scientific, USA). After denaturation protein lysates were separated on gradient SDS polyacrylamidegels (Mini-PROTEAN TGX Precast Gels, Any kDa, BioRad, Germany) and transferred to nitrocellulose membranes (0.2 μm, Amersham, USA) at 4 °C overnight. Equal loading of 40 μg/lane and transfer of proteins was confirmed by staining of membranes with Ponceau S solution (Sigma-Aldrich). Nonspecific protein binding was blocked by incubation in 5% non-fat milk powder, 0.1% Tween in TBS (TBST) followed by incubation with the primary antibodies, i.e. anti-myelin basic protein (MBP, 1:15,000, Covance, USA), anti-microtubuli associated protein-2 (MAP-2, 1:1000, Sigma-Aldrich), anti-NeuN (1:2000, Millipore), anti-Olig2 (1:1000, Millipore) and anti-beta Actin (1:10,000, Sigma-Aldrich) in blocking solution at 4 °C overnight. Afterwards, membranes were incubated with the appropriate peroxidase-conjugated secondary antibody at room temperature for 1 h (rabbit anti mouse 1: 5000, Dako, Denmark) in blocking solution followed by Chemiluminescent detection with the ECL prime western blotting detection reagent (Amersham, GE Healthcare Life Science, USA). For visualization and densitometric analysis the ChemiDocXRS+ imaging system and ImageLab software (Bio-Rad, Germany) were used.

2.4. Behavioral assessment

Behavioral testing was initiated in juvenile animals on PND 30 and repeated on PND 44 in young adult animals. From PND 21 on animals were transferred to an inversed 12 h light: 12 h dark cycle. Testing was started with one day of elevated plus maze followed by one day open field and one day novel object recognition test. Data were recorded using an automatic tracking system (Video-Mot2, TSE Systems, Germany) and exported for statistical analysis. After a recovery period of three days mice were tested for sensorimotoric functions in the Rota Rod test. All experimental procedures were carried out in the dark phase in a dimly lit (red light) and a low noise environment (behavioral unit) by a single investigator blinded to the experimental groups.

The elevated plus maze (EPM) was used for the assessment of locomotor and anxiety/exploration-related behavior (Lister, 1987; Walf and Frye, 2007). It is raised 500 mm off the ground and consists of two facing open arms and two facing closed arms (both 300 mm × 50 mm, 150 mm high enclosement), extended from a central platform. For testing, mice were placed on the central platform and behavior was recorded for 5 min. The time spent in the open and closed arms was measured (Walf and Frye, 2007). The open field test was used to evaluate spontaneous motor- and rearing activity as well as to assess anxiety/exploration-related behavior (Milner and Crabbe, 2008) Animals were placed into the center of an open field arena (55 × 55 × 50 cm) on infrared (IR) translucent material, placed upon an infrared light-box (850 nm, TSE Systems) to increase contrast for video recording. Movements were recorded by the tracking system for 5 min. Activity parameters, i.e. traveled distance and velocity were analyzed and anxiety/exploration-related behavior was assessed by calculation of the percentage of time the animal stayed in the central area of the box in relation to the total time spent in the arena. Rearing activity was calculated as the time the animals reared in the border region relative to the total time the mice spent in this region. Changes of sensorimotoric behavior were analyzed in the Rota Rod test consisting of a rotating drum with a speed accelerating from 4 to 40 rpm (Ugo Basile, Italy) within 120 s, which allows assessing motor coordination skills. The time the animal can run on the drum was quantified (maximum testing time 120 s). The novel object recognition (NOR) task is a non-spatial, non-aversive memory test which relies on the observation, that animals preferentially explore novel objects over those that are familiar. This preference serves as an indicator for memory formation (Bevins and Besheer, 2006). Testing was performed in the open field arena one day after the open field. In the initial familiarization trial, animals were placed in the open field arena, where 2 identical objects as new cues are located in two facing corners. The behavior was recorded for 5 min and the animals' object exploration activity was measured. Afterwards, the animals were returned to their cages for an inter-trial interval of 30 min. In the following retention/test trial, animals were exposed to one familiar object and one novel object replacing the second familiar object in the arena. Again, behavior and object activity were recorded for 5 min. Total object activity and novel object activity were measured.

2.5. Statistical analysis

All results were expressed as box plots including median values, the 25% and the 75% percentile. Sample size for analysis of treatment effects by HT was determined a priori using G*Power (version 3.1). For both, histological brain injury and long-term functional deficits an α-level of 0.05 and a power of 0.8 were required. Based on previous reports (Carlsson et al., 2012; Liu et al., 2013; Patel et al., 2015) a Cohen's d ES of 0.6 and 0.5 was used for histological brain injury and functional deficits, respectively. A mortality of 15% was assumed for the selected HIE model. This yielded a final sample size of 12 (histological brain injury)

and 15 (functional deficits) animals per group. Effects of intra-hypoxic temperature and the level of hypoxia on brain injury were analyzed in an explorative way without performing a 'pre-study' sample size calculation. For statistical analysis, the GraphPad Prism 6.0 software package (GraphPad Software) was used. Data were tested for Gaussian distribution with the D'Agostino and Pearson omnibus normality test and then analyzed either by ordinal 1-way ANOVA or by Kruskal-Wallis (non-parametric) with post hoc Bonferroni correction for multivariate analyses or with Dunn multiple comparison tests, respectively. If 2 groups were compared, unpaired, two-tailed Student *t*-test or Mann Whitney test (non-parametric) was applied. In all analyses, $p < 0.05$ was considered statistically significant.

3. Results

3.1. Modeling hypoxic-ischemic encephalopathy (HIE) is associated with a significant drop in body core temperature thereby reducing HIE-induced brain injury

To define target temperature values for modeling of HIE and therapeutic hypothermia (HT) we first measured the physiological (i.e. nesting) temperature of PND 9 mice resulting in a mean temperature of 35.2 ± 0.5 °C (Fig. 1A). To exclude confounding effects of reduced warming by the dam after surgery additional measurements were performed immediately before hypoxia or normoxia in sham-operated and

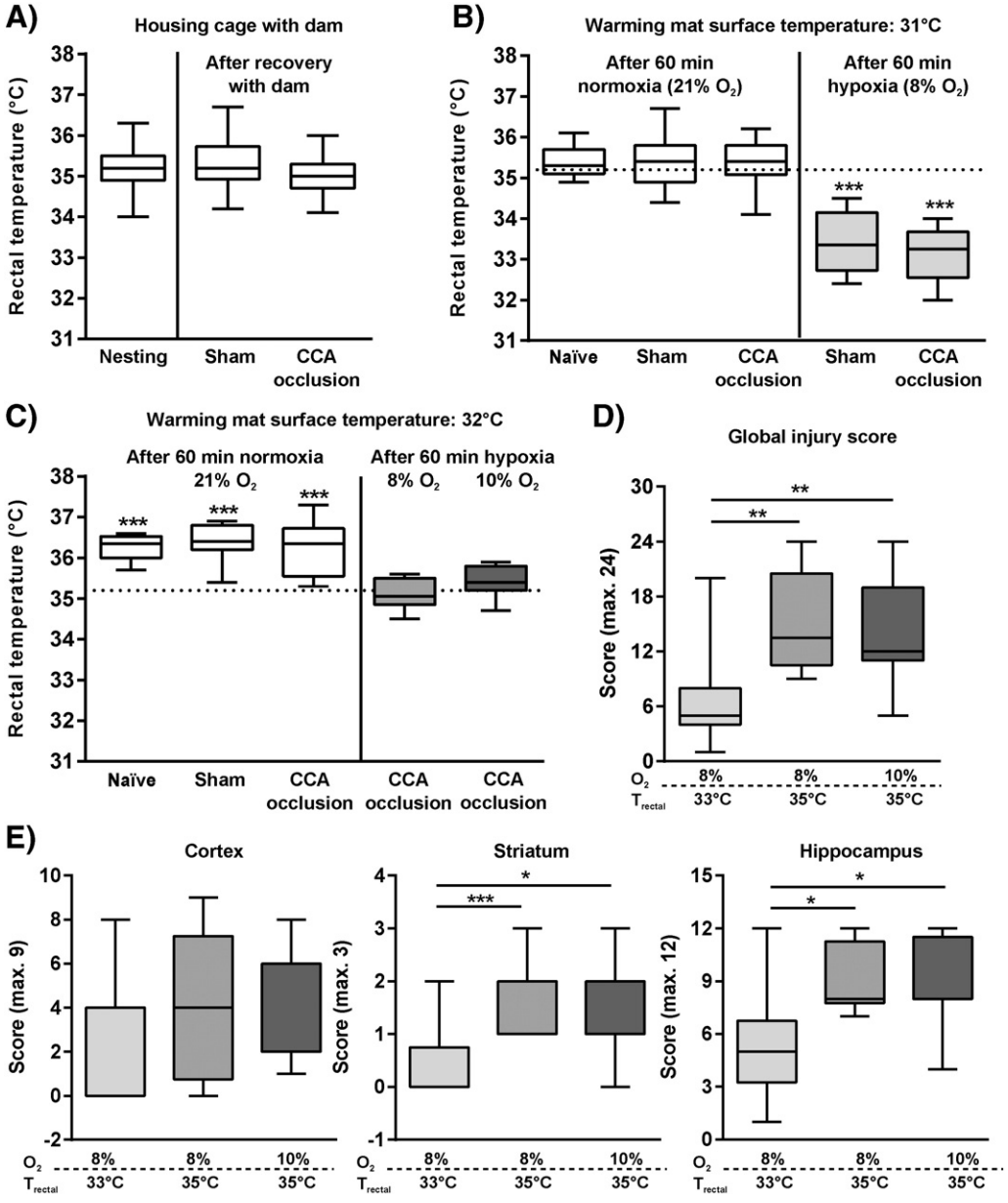

Fig. 1. Modeling hypoxic-ischemic encephalopathy (HIE) in neonatal mice is associated with a significant reduction in body core temperature resulting in reduced brain injury. The rectal temperature of postnatal day 9 C57BL/6 mice was measured immediately when pups were removed from their dam (Nesting, $n = 94$) and after a recovery period of 60 min with their dam following sham operation and CCA occlusion, i.e. immediately before hypoxia or normoxia (A). Rectal temperatures of naïve ($n = 15$), sham-operated ($n = 20$) and CCA-occluded mice ($n = 23$) were determined after 60 min normoxia (21% O_2) or hypoxia (8% O_2) on a warming mat set to 31 °C surface temperature (B). To maintain nesting temperatures during hypoxia the warming mat temperature was increased by 1 °C and naïve ($n = 10$), sham-operated ($n = 10$) and CCA-occluded ($n = 10$) mice were exposed to normoxia (21% O_2) (C, white boxes). Applying the same ambient temperature CCA-occluded mice were exposed to 60 min hypoxia at 8% O_2 ($n = 10$) or 10% O_2 ($n = 11$) (C, gray boxes). Dotted lines in (B) and (C) indicate the median nesting temperature (*** $p < 0.001$ vs. nesting). Neuropathological assessment was performed on cresyl violet stained 20 μm cryostat sections of PND 16 mice exposed to hypoxia-ischemia (i.e. CCA-occlusion plus hypoxia) on PND 9 at the indicated conditions (D, E). Total (D) and regional (E) neuropathological scores were determined ($n = 10$–11/group). *$p < 0.05$, **$p < 0.01$. ***$p < 0.001$.

CCA-occluded animals after a recovery period of 60 min with their dams revealing temperatures comparable to the mean nesting temperature (Sham: 35.3 ± 0.6 °C, CCA-occluded: 35.0 ± 0.4 °C, Fig. 1A). Next, naïve mice were exposed to 60 min of normoxia (21 °C) on a warming mat set to a surface temperature of 31 °C resulting in similar rectal temperatures (Fig. 1B). To test whether the surgery intervention and/or anesthesia influences endogenous thermoregulation in neonatal mice, sham-operated as well as CCA-occluded mice were exposed to normoxia using the same experimental set up leading to rectal temperatures comparable to the nesting temperature (Fig. 1B). Based on these initial measurements sham-operated and CCA-occluded mice were exposed to hypoxia at 8% O_2 for 60 min resulting in a significant drop of body core temperature to 33.4 ± 0.8 °C and 33.1 ± 0.7 °C, respectively (further indicated as T_{rectal} 33 °C, Fig. 1B). To ensure that this drop was truly central and not due to a general degradation of hemodynamics we performed heart rate measurements to record the physiological status. Control animals, i.e. naïve, sham-operated and CCA-occluded mice at normoxia and nesting body core temperature, revealed heart rates comparable to previously published physiological values for p6/p7 mice (Zehendner et al., 2013). CCA-occluded animals exposed to hypoxia at the same warming mat temperature did not reveal significant reductions in heart rates suggesting that endogenous cooling under these conditions cannot be attributed to a hemodynamic collapse (Supplementary Fig. 2).

Considering the clinical situation in human infants (neonates most likely have physiological temperatures during the acute intrapartum insult), we aimed to keep the animals' temperature constant at the level of the nesting temperature during hypoxia through increasing the warming mat temperature by 1 °C. As expected, naïve, sham-operated and CCA-occluded mice revealed significantly increased rectal temperatures after 60 min in normoxia at a warming mat surface temperature of 32 °C (Fig. 1C). In contrast, animals exposed to hypoxia (8% O_2) at the same warming mat temperature demonstrated a mean rectal temperature of 35.1 ± 0.4 °C which is comparable to the nesting body core temperature (Fig. 1C). However, mortality increased to 48.8% compared to 8.3% at T_{rectal} 33 °C and 8% O_2. Therefore, the hypoxic stimulus was reduced to 10% O_2 leading to rectal temperatures comparable to physiological levels at normoxia (35.4 ± 0.4 °C, further indicated as T_{rectal} 35 °C, Fig. 1C); and mortality declined to 15.4%.

To evaluate the individual impact of temperature and level of hypoxia on HIE-induced brain injury we assessed neuropathological changes on cresyl violet stained brain tissue sections (Fig. 1D). Injury scores were significantly increased in those experimental groups where rectal temperatures were maintained at the nesting temperature (i.e. T_{rectal} 35 °C 10% O_2 and T_{rectal} 35 °C 8% O_2) compared to the group with endogenous intra-hypoxic cooling (i.e. T_{rectal} 33 °C 8% O_2, Fig. 1D). These differences became particularly evident in the striatum and the hippocampus (Fig. 1E). Hypoxia at T_{rectal} 33 °C and 8% O_2 resulted in rather mild brain injury with a significant amount of mice that developed no injury in different brain regions, e.g. 58% in the cortex and 75% in the striatum (Fig. 1E). No significant differences were detected between 8% O_2 and 10% O_2 at T_{rectal} 35 °C. However, due to the high mortality rate the experimental group 8% O_2 T_{rectal} 35 °C was excluded from further analysis.

3.2. Maintenance of the nesting temperature during HIE induces significant gray and white matter damage accompanied by oligodendrogenesis and astrogliosis

Based on the preceding findings two HIE models, i.e. CCA-occlusion plus hypoxia at T_{rectal} 33 °C 8% O_2 and CCA-occlusion plus hypoxia at T_{rectal} 35 °C 10% O_2 were compared with respect to gray and white matter injury. Western blot analyses of MAP-2 and MBP expression at the level of the striatum and at the level of the hippocampus demonstrated a significant loss of both axonal and myelin structures in ipsilateral hemispheres of animals exposed 10% O_2 at T_{rectal} 35 °C. In contrast, mice exposed to 8% O_2 at T_{rectal} 33 °C showed MAP-2 and MBP protein levels equivalent to sham-operated mice (Fig. 2). In accordance to reduction of axonal structures (MAP-2, Fig. 2B,E) expression of the neuronal cellular marker NeuN was significantly decreased in mice exposed to 10% O_2 at T_{rectal} 35 °C compared to 8% O_2 at T_{rectal} 33 °C (Fig. 2A,B,D,E). Interestingly, Olig2 as a pan-cellular marker for oligodendrocytes remained either unchanged (Fig. 2C) or significantly increased (Fig. 2F) whereas myelin structures demonstrated by MBP expression were reduced in the model of moderate to severe HIE-induced brain injury (i.e. 10% O_2 at T_{rectal} 35 °C, Fig. 2C,F).

To more specifically define cellular responses we performed immunohistochemical staining of NeuN and Olig2 (Fig. 3A,B). In addition to neurons and oligodendrocytes, astroglia have been suggested to be involved in degenerative but also regenerative processes associated with neonatal HIE pathogenesis (Romero et al., 2014; Gelot et al., 2008). Therefore, we included analysis of GFAP as a marker of reactive astrogliosis (Fig. 3C). Since neither neuronal nor oligodendrocyte and astrocyte density were modulated in contralateral hemispheres (Supplementary Fig. 3), values of ipsilateral hemispheres were related to contralateral values for group comparisons. The most significant reduction of neuronal density was observed in the hippocampus in both models ($p < 0.05$ vs. 100%). However, neuronal loss was significantly elevated at T_{rectal} 35 °C 10% O_2 compared to T_{rectal} 33 °C 8% O_2 (Fig. 3A). In the striatum neuronal density was significantly reduced at T_{rectal} 35 °C 10% O_2 ($p < 0.01$ vs. 100%) but not at T_{rectal} 33 °C 8% O_2 ($p > 0.05$ vs. 100%, Fig. 3A). HI-induced regional decrease in neuronal density was accompanied by an increase in oligodendrocyte cellularity depending on severity of injury, evident in the striatum and hippocampus (Fig. 3B). Immunohistochemical co-staining of the proliferation marker Ki67 combined with NeuN and Olig2 in two adjacent sections (20 μm distance) revealed that HI-induced alleviation in oligodendrocytes is most probably a result of an increased proliferation (Supplementary Fig. 4). In contrast to oligodendrocyte density, astroglia responses measured by GFAP density were significantly increased in both models and in all regions analyzed, independent of the severity of the insult ($p > 0.05$ vs. 100%, Fig. 3C). Nevertheless, increased HIE-induced brain injury at T_{rectal} 35 °C 10% O_2 was associated with an overall increased astrogliosis compared to T_{rectal} 33 °C 8% O_2 which, however, did not correlate with the degree of local neuronal injury (Fig. 3A,C).

3.3. Early neuroprotection by therapeutic hypothermia is locally restricted and dependent on therapy onset

Based on our findings we used the model, in which maintenance of the nesting body core temperature during 60 min of hypoxia at 10% oxygen results in low mortality and significant brain injury to assess therapeutic effects of HT either started immediately or with a 2-h-delay after hypoxia. Measurements of body core temperatures in both experimental settings showed that in the normothermia (NT) control group physiological rectal temperatures were maintained until the end of intervention with an average temperature of 35.1 ± 0.5 °C (immediate onset, Fig. 4A) and 35.3 ± 0.5 °C (delayed onset, Fig. 4B). Animals of the HT group were cooled to an average body core temperature of 32.2 ± 0.7 °C (immediate onset, Fig. 4A) and 32.4 ± 0.8 °C (delayed onset, Fig. 4B) resulting in a target temperature difference of approximately 3 °C similar to the first pre-clinical hypothermia study in neonatal C57BL/6 mice (Carlsson et al., 2012). Sham-operated normoxic control mice left with their dams revealed rectal temperatures comparable to the nesting temperature of naïve mice and of NT control mice (Fig. 4A, B). Of note, in the delayed HT group we detected significantly reduced rectal temperatures in HIE mice compared to sham mice at the onset of therapeutic temperature intervention, i.e. 2 h after recovery with the dam (Fig. 4B). Acute weight gain within the first two days was not affected by the different temperature interventions (Supplementary Fig. 5A). Since the onset of NT had no impact on total and regional brain injury (Supplementary Fig. 5B) animals of immediate and delayed NT

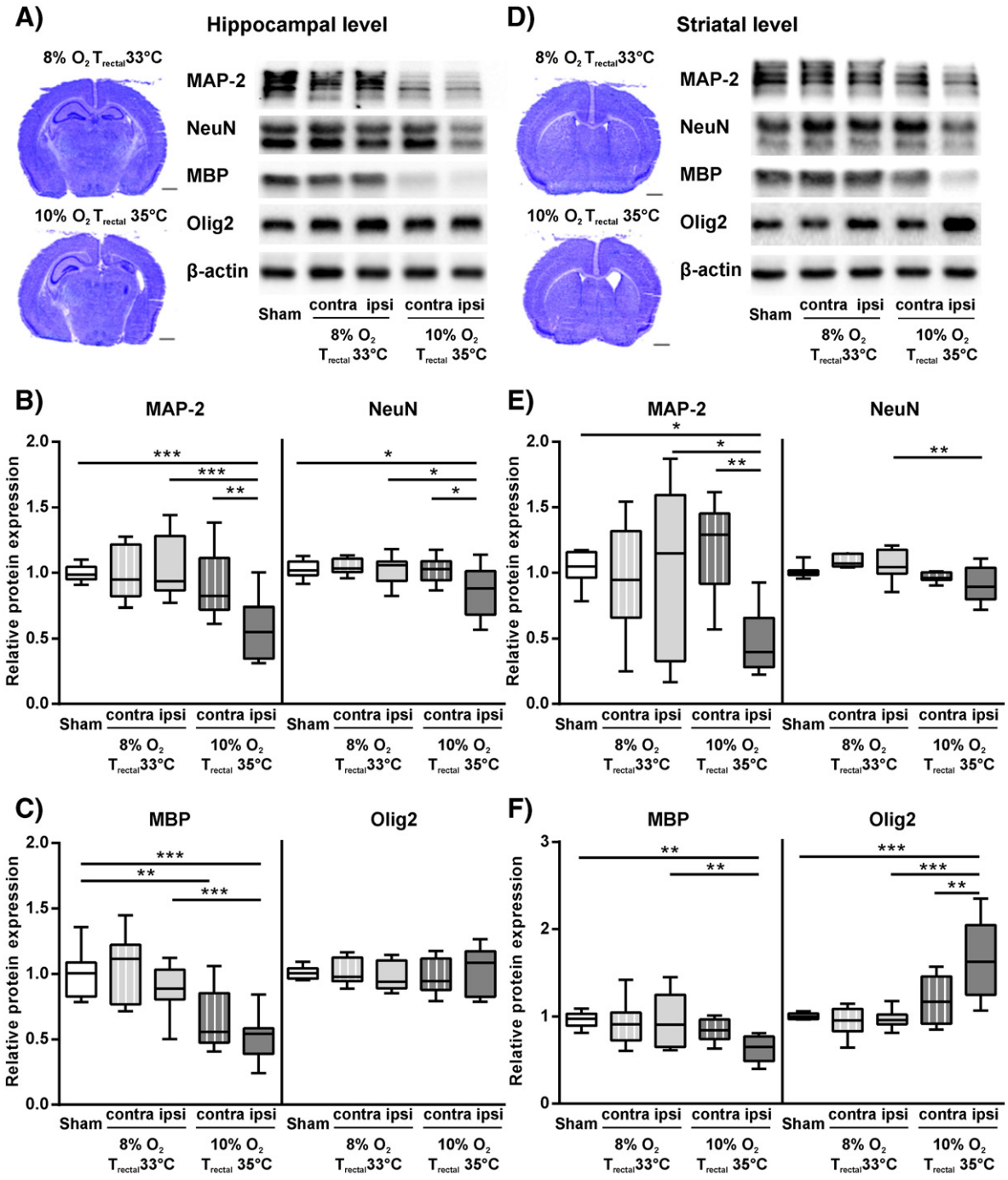

Fig. 2. Maintenance of the nesting temperature during HIE modeling induces significant gray and white matter injury. Postnatal day (PND) 9 C57BL/6 mice were exposed to hypoxia-ischemia at 8% or 10% oxygen and a rectal temperature of 33 °C and 35 °C, respectively. Protein lysates were isolated from 8 × 20 μm cryostat tissue sections between −1.9 mm and −2.3 mm from bregma (hippocampal level, A-C) and between 0.5 mm and 0 mm from bregma (striatal level, *D*-F). Western blot analyses was applied to quantify expression of microtubuli associated protein-2 (MAP-2), NeuN, myelin basic protein (MBP) and Olig2. Data were normalized to the reference protein β-Actin and sham-operated controls. $n = 9$–10/group, Scale bar in (A) and (D): 1 mm $^{*}p < 0.05$, $^{**}p < 0.01$, $^{***}p < 0.001$.

were pooled in the following analyses (Fig. 4C–F). Neuropathological assessment revealed that overall and local cortical tissue injury was reduced by both HT treatments even though significant differences were detected only for immediate HT (Fig. 4C). Significant differences were observed for both treatment modalities in the hippocampus but not in the striatum (Fig. 4C, D). Hippocampal neuronal density was significantly increased by HT, independent of therapy onset (Fig. 4D) whereas HIE-induced oligodendrogenesis and astrogliosis were not significantly modulated by either protocol (Fig. 4E, F).

Therapeutic hypothermia partially restores motoric functions, exploratory behavior and histological outcome while anxiety-related behavior and cognitive deficits remain unchanged.

Based on previous reports (Bona et al., 1998; Burnsed et al., 2015; Trescher et al., 1997) describing that HT-induced acute neuroprotection does not necessarily translate into long-term protection from functional deficits we applied a battery of behavioral tests to assess locomotor activity, anxiety/exploration-related behavior and cognitive function. Potential confounding effects by different weights due to neonatal HIE

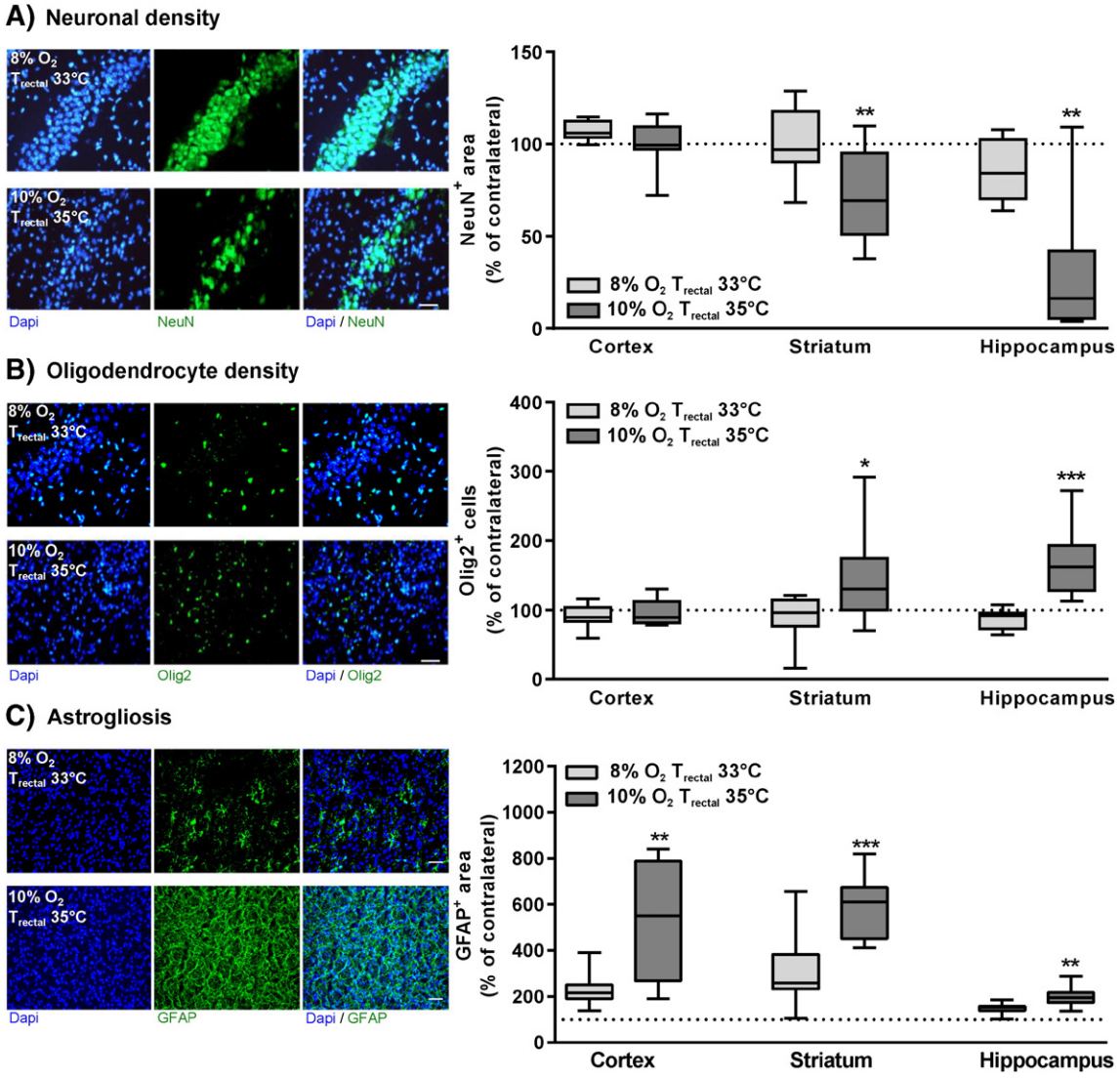

Fig. 3. HIE-modeling at nesting temperature results in local neuronal loss coinciding with oligodendrogenesis and reactive astrogliosis. Neuronal (A) and oligodendrocyte (B) density as well as astrogliosis (C) were determined by immunohistochemistry for NeuN, Olig2 and GFAP, respectively. Analysis was carried out in the cortex, striatum and hippocampus of PND16 mice after exposure to hypoxia-ischemia at 8% or 10% oxygen and a rectal temperature of 33 °C or 35 °C at PND9. Representative images are derived from the CA3 region of the ipsilateral hippocampus (A and B) and from the ipsilateral striatum (C). Astrogliosis and cellular density of neurons and oligodendrocytes were quantified by measuring the NeuN (A) and GFAP (C) positive area and by counting Olig2-positive cells (B) in 3 non-overlapping regions of interest per brain region ($n = 9$–11/group). The dotted line in (C) indicates 100%. Scale bar: 50 μm in (A) and (B), 100 μm in (C). $^{*}p < 0.05$, $^{**}p < 0.01$, $^{***}p < 0.001$ vs. 8% O_2 T_{rectal} 33 °C.

and/or HT could be excluded because animals revealed a similar weight gain across all experimental groups throughout the testing period (Supplementary Fig. 6). Behavioral performance of HIE mice was independent of immediate or delayed onset of NT (Supplementary Table 2). Therefore, animals of both control groups were pooled for analysis. Locomotor and anxiety-related behavior was assessed in the elevated plus and the open field maze at 3 and 5 weeks post HIE. Neither HIE nor HT modulated locomotor activity of juvenile and young adult mice (Supplementary Fig. 7A-D). However, neonatal HIE independent of HT induced a strong and persistent alteration of anxiety/exploration-related behavior, measured as significantly increased time intervals that the animals spent in open arms, coinciding with reduced time periods in closed arms (Fig. 5A–C). To verify these observations mice were exposed to the open field maze revealing no significant differences in the time period the mice spent in the central region of the maze among all tested groups (Supplementary Fig. 7E). Nevertheless, vertical activity (i.e. rearing) in the border region of the open field maze was significantly reduced by HIE which was restored by immediate HT at 3 weeks post HIE and by both HT protocols at 5 weeks post HIE (Fig. 5D). Since reduced rearing behavior may be associated with motoric dysfunctions we further evaluated sensorimotoric function in the accelerated Rota Rod test thereby confirming that HIE-induced alterations in motoric functions were ameliorated by immediate but not by delayed HT in juvenile HIE mice although the significant protective effect disappeared in young adult mice (Fig. 5E). Directed exploration and cognitive function was assessed in the novel object recognition test, demonstrating a reduced exploratory activity expressed as the time the mice spent with two unknown objects in the open field arena during the familiarization/habituation session (Fig. 5F and G). This reduced exploration activity was transiently improved by immediate but not by delayed HT (Fig. 5G). By replacement of one of the familiar objects with a new object, cognitive function was assessed revealing a reduced novel object activity in young adult HIE mice even though neither immediate nor delayed HT significantly improved recognition (Fig. 5H). Whether partial HT-induced functional improvements and early neuroprotection translate into long-term tissue protection was assessed by measurement of brain atrophy demonstrating that except of the hippocampus, which was protected by immediate HT, overall brain atrophy and cortical as

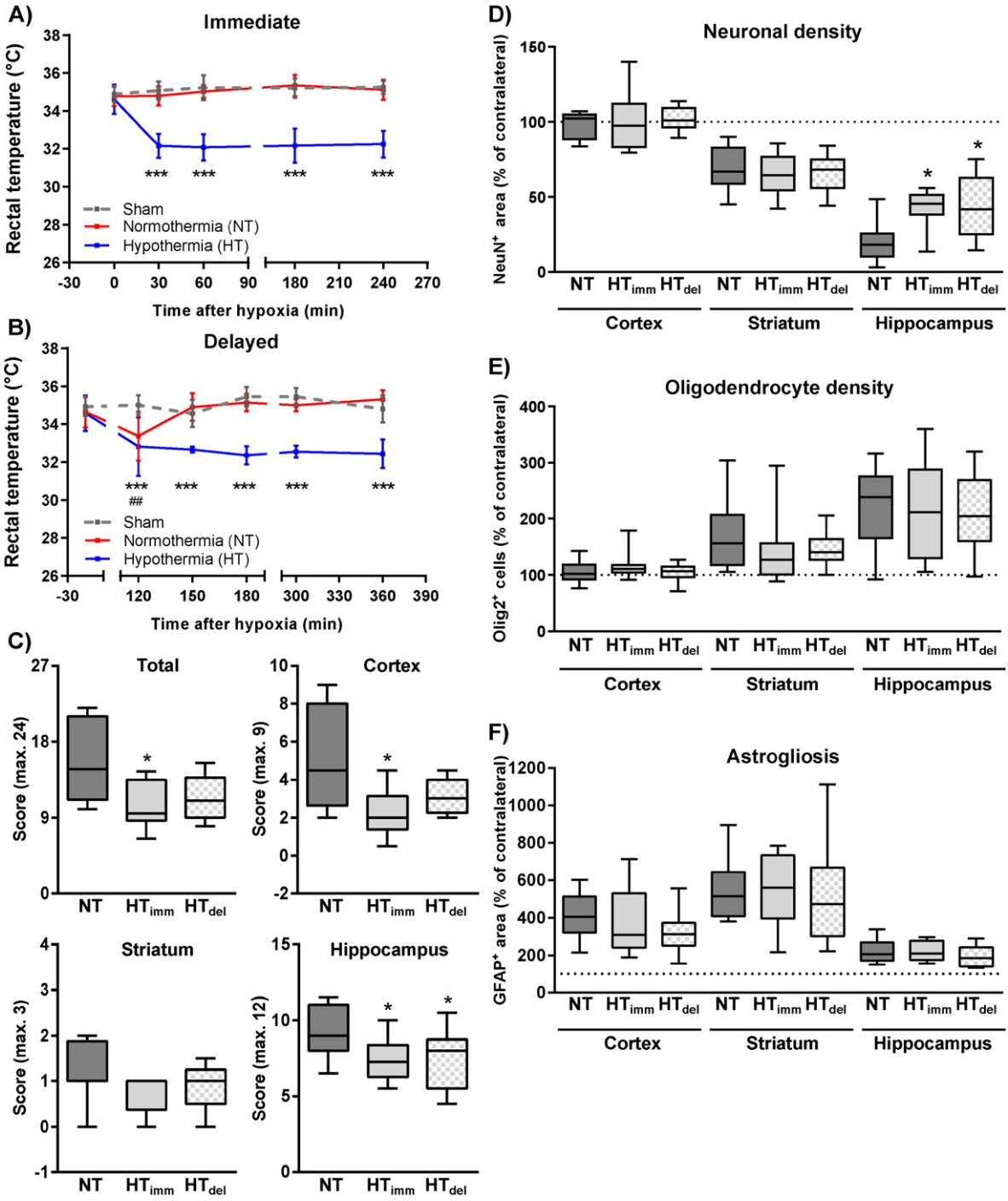

Fig. 4. Therapeutic hypothermia confers early locally restricted neuroprotection. Histological brain injury was determined on 20 μm cryostat sections of PND 16 mice that were exposed to hypoxia-ischemia (10% O_2, T_{rectal} 35 °C) followed by HT at 27 °C (plate surface) started immediately (A) or with a delay of 2 h (B) on PND9. In the delayed therapy paradigm pups were placed back to their dam between HIE and therapy. Control mice (Normothermia) were exposed to a warming mat to maintain nesting temperatures (A, B). Neuropathological assessment was performed on cresyl violet stained tissue sections and total as well as regional injury scores were quantified (C). Neuronal (D), oligodendrocyte (E) density and astrogliosis (F) were determined by immunohistochemistry for NeuN, Olig2 and GFAP in the cortex, striatum and hippocampus (n = 10–12/group). NT = normothermia, HT_{imm} = immediate hypothermia, HT_{del} = delayed hypothermia. $^{***}p < 0.001$ HT vs. Sham, $^{\#\#}p < 0.001$ NT vs. Sham, $^{*}p < 0.05$ vs. NT.

well as striatal tissue loss were not modulated by therapeutic HT, independent of protocols (Fig. 6).

4. Discussion

In the current study we show that endogenous thermoregulatory responses to hypoxia-ischemia in neonatal mice are associated with pronounced neuroprotection. Using the most clinically relevant HIE model (i.e. maintaining the nesting temperature during the insult), we demonstrate significant short-term protection from HIE-induced brain injury with slight advantages of an immediate over delayed onset of therapeutic hypothermia (HT). However, long-term tissue loss and functional deficits were only partially restored.

A critical and often unknown issue in many translational hypothermia studies is the nesting temperature and the rationale for selection of target temperatures. We determined a nesting temperature of 35.2 ± 0.5 °C which was significantly below the previously suggested physiological temperature of 36 °C (Barnett and Walker, 1974;

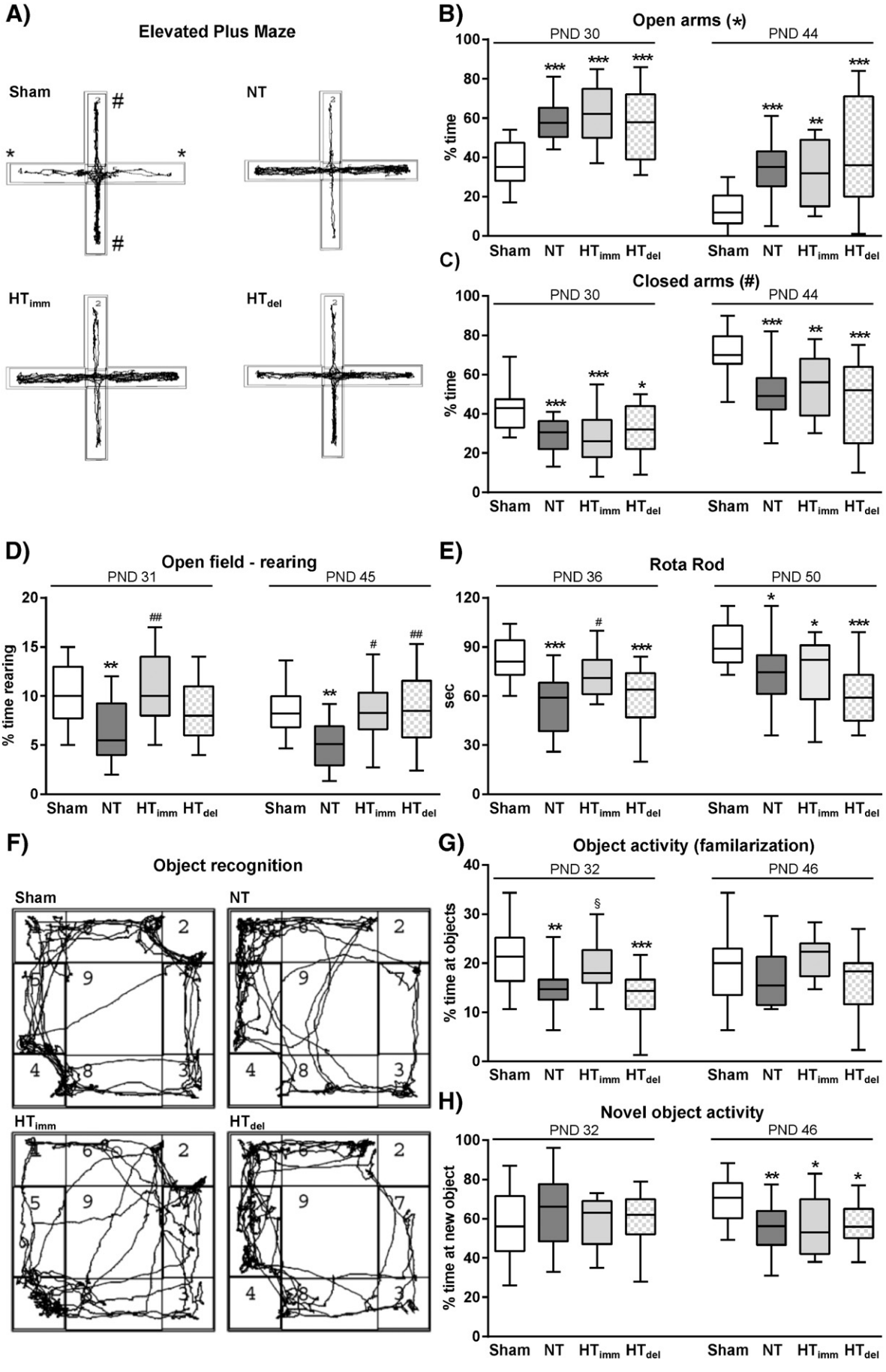
A)
Elevated Plus Maze
Sham
NT
HTimm
HTdel
B)
Open arms (*)
PND 30
PND 44
% time
Sham NT HTimm HTdel
C)
Closed arms (#)
D)
Open field - rearing
PND 31
PND 45
% time rearing
E)
Rota Rod
PND 36
PND 50
sec
F)
Object recognition
G)
Object activity (familarization)
PND 32
PND 46
% time at objects
H)
Novel object activity
% time at new object

Burnsed et al., 2015; Carlsson et al., 2012) affirming the need of study-specific systematic rectal temperature monitoring which has largely been ignored in previous studies. Only few studies provide pre-surgery and pre-hypoxia rectal temperatures with values approximately 2–3 °C below the rectal temperature measured after hypoxia in warm chambers (Barks et al., 2010; Bona et al., 1998; Liu et al., 2004). Since nesting temperatures are often not recorded it is difficult to dissect whether reduced pre-hypoxia/pre-surgery values in previous studies might have been caused by the operational procedures or whether animals have been heated to non-physiological artificial temperatures during hypoxia. The present study demonstrates that animals independent of the surgical intervention (i.e. sham or CCA occlusion) are capable of maintaining physiological (i.e. nesting) temperatures under normoxia while hypoxia results in a significant endogenous drop in body core temperature. These findings suggest that an endogenous compensatory thermoregulation occurs, which limits brain injury induced by the hypoxic event. Our physiological data (i.e. heart rate) further support that this drop in temperature was endogenously controlled and not a consequence of general deterioration of hemodynamics. Since neonatal encephalopathy is a result from acute intrapartum hypoxia, neonates are supposed to have physiological temperatures during the acute insult. Therefore, we decided to maintain the nesting rectal temperature during modeling the insult leading to significant brain injury affecting gray and white matter structures and cells.

A limitation of the present study is that due to technical limitations intra-cerebral temperatures could not be recorded to entirely exclude unexpected heating of the CNS when maintaining the nesting temperature during hypoxia. However, the rectal temperature has been shown to correlate well with brain temperature in neonatal rodents (Thoresen et al., 1996). Furthermore, the heart rate of animals exposed to HIE at nesting rectal temperatures did not significantly differ from normoxic controls. Even though we aimed to determine the effect by temperatures and levels of hypoxia separately, a final conclusion cannot be drawn because of high mortality rates at 8% O_2 and nesting rectal temperature, which may have led to arbitrary selection of animals. This is supported by the fact that these animals had similar injury scores as animals at 10% O_2 at the same rectal temperature.

The present study is of particular interest regarding critical care in humans because it supports current clinical practice where passive cooling during resuscitation is anecdotally recognized to enhance therapeutic outcome. Moreover clinical hypothermia trials provide first indications that babies receiving standard care alone undergo a natural cooling (Robertson et al., 2008). Thus, it was suggested that the 'dilution of the hypothermic effect' needs to be considered in future trials because natural cooling could be an endogenous neuroprotective response (Jayasinghe, 2015; Robertson et al., 2008). Indeed, our results demonstrate that endogenous cooling confers profound neuroprotection by reducing injury which was well described by reduced neuropathological alterations, by a reduced loss of gray and white matter structures and a decreased neuronal loss. Of note, oligodendrocyte cellularity, quantified by immunohistochemistry and western blot analysis, increased especially in severely affected brain regions which might be explained by compensatory oligodendrocyte proliferation as previously described (Dizon et al., 2010; Kako et al., 2012; Xiong et al., 2013). Moreover,

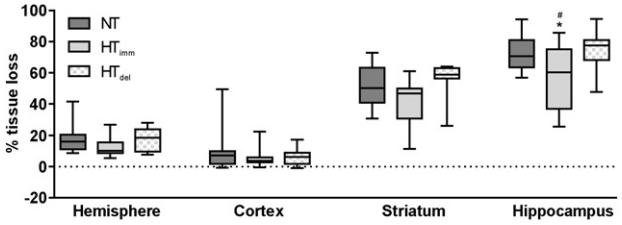

Fig. 6. HIE-induced long-term brain tissue loss is partially protected by immediate but not by delayed therapeutic hypothermia. Brain atrophy was determined on cresyl violet stained brain tissue sections of PND 51 mice exposed to hypoxia-ischemia (10% O_2 T_{rectal} 35 °C) followed by normothermia or hypothermia on PND 9. Intact areas were measured at a distance of 400 μm between +1 mm and −2.6 mm from bregma. Volumes were calculated for total hemispheres and the indicated brain regions. Tissue loss was expressed as the percentage of volume reduction compared to intact contralateral volumes (n = 11–18/group). NT = normothermia, HT_{imm} = immediate hypothermia, HT_{del} = delayed hypothermia. $^{*}p < 0.05$ vs. NT, $^{\#}p < 0.05$ vs. HT_{del}.

HIE led to increased astrogliosis even after mild brain injury which was also prominent in regions (e.g. cortex) without neuronal cell loss. However, at the selected time point (i.e. 7 days post HIE), quantification of $GFAP^{+}$ areas may rather reflect reactive astrogliosis and/or glial scar formation as described for different adult brain injury models (Sofroniew, 2009) than providing direct evidence for cellular responses. Nevertheless, astrocytes are supposed to exert multiple effects including exacerbation of brain injury but also promotion of regenerative processes (Romero et al., 2014; Gelot et al., 2008). Therefore, further research should focus on the temporal and spatial dynamics of different cell types, their function and interaction in HIE-induced pathology to identify new therapeutic targets.

Despite the huge body of pre-clinical studies aiming at the identification of preferred HT treatment protocols a consensus is still missing, particularly for neonatal mice where only few studies have been published. Out of eight reports five can hardly be translated into the clinical setting either because of young age, i.e. PND 3–7 (Kida et al., 2013; Liu et al., 2013; Wang et al., 2014) rather corresponding to preterm babies where cooling is not recommended or because of exogenously applied cooling during hypoxia (Lin et al., 2014; Zhu et al., 2006). The latter is also of limited translational value because the acute intrapartum hypoxic event occurs before cooling can be applied. The remaining three studies conducted HIE and therapeutic HT in PND 9–10 mice (Burnsed et al., 2015; Carlsson et al., 2012; Griesmaier et al., 2014) suggested to be the term-equivalent of human brain development (Semple et al., 2013). Using this model we confirmed neuroprotection at 7 days post HIE elicited by a 4-h HT therapy immediately after HIE (Burnsed et al., 2015; Carlsson et al., 2012). However, a delay of 2 h for the same treatment reduced therapeutic efficacy while the hippocampus was still protected which is in contrast to previous studies demonstrating a complete loss of protection by a similar delayed HT protocol (Carlsson et al., 2012; Griesmaier et al., 2014). This may be explained by differences in mouse strains (Griesmaier et al., 2014) and by inter-experimental differences in injury severity caused by analysis of immediate and delayed treatment in separate experiments (Carlsson et al., 2012). In the current study we performed a systematic analysis, randomly distributing pups

Fig. 5. Motoric functions and exploratory behavior are partially restored by therapeutic hypothermia without affecting anxiety-related behavior and cognitive deficits. Behavioral testing was initiated in juvenile animals on PND 30 that were either sham-operated or exposed to hypoxia-ischemia (10% O_2, T_{rectal} 35 °C) followed by normothermia or hypothermia on PND9. Testing was started with the elevated plus maze, followed by the open field test the next day and the novel object recognition task the day after. Rota Rod performance was analyzed after a break of 3 days. This test series was repeated after 2 weeks starting on PND 44. On the first day mice were placed on the central platform of the elevated plus maze and behavior was recorded for 5 min (A–C). The time spent in the open and closed arms was measured and is expressed as % time of total test time (B, C); representative tracking recordings are shown in (A). For the open field test animals were placed into the center of an open field arena and movements were recorded by the tracking system for 5 min. Rearing activity was analyzed by calculation of the time the animals reared in the border region relative the total time the mice spent in this region (D). Changes of sensorimotoric behavior were analyzed in the Rota Rod test consisting of a rotating drum with a speed accelerating from 4 to 40 rpm within 120 s (maximal testing time). The time the animal runs on the drum was quantified (E). For the novel object recognition (NOR) test animals were placed in the open field arena with 2 identical objects as new cues located in two facing corners; objects were located at positions 2 and 4 (F). Movements during this familiarization session were recorded for 5 min and the percentage of time the mice spent with both objects of total test time was calculated (G). In the second, i.e. the novel object recognition session, animals were exposed to one familiar object and one novel object replacing the second familiar object in the arena. Object activity was recorded for 5 min and the percentage of time the mice spent with the new object of the total object time was analyzed (H). n = 15–22/group. NT = normothermia, HT_{imm} = immediate hypothermia, HT_{del} = delayed hypothermia. $^{*}p < 0.05$, $^{**}p < 0.01$, $^{***}p < 0.001$ vs. Sham, $^{\#}p < 0.05$, $^{\#\#}p < 0.01$ vs. NT, $^{\S}p < 0.05$ vs. HT_{del}.

per litter and experiment across all experimental groups reducing a potential bias due to inter-experimental and/or litter-specific variations.

The regional variability of HIE injury is well known. However, there is less agreement on a selective protection of specific brain regions by HT. Confirming two previous reports in neonatal mice (Burnsed et al., 2015; Carlsson et al., 2012) we observed a strong protection in hippocampus and cortex but not in the striatum after brief mild HT started immediately after HIE. Using a similar treatment paradigm in neonatal rats the hippocampus was not protected which might be attributed to species differences but also to pre-selection of animals, i.e. mildly affected animals were excluded from regional analysis (Patel et al., 2015). We did not categorize experiments into degrees of injury because individual responses might have contributed to the well described variation in pathology. This also reflects the clinical situation where neonates with similar insults have varying outcomes (Yager and Ashwal, 2009). Regional differences might not only be explained by different apoptotic mechanisms (Northington et al., 2011; Northington et al., 2007) but also by a spatial–temporal regulation of pathophysiological processes during the evolution of HIE. This is supported by our results showing that endogenous cooling during hypoxia results in protection of mainly affected regions such as cortex, striatum and hippocampus. However, therapeutic cooling after hypoxia protected only the hippocampus and the cortex; and a delay of treatment further abrogated protection in the cortex, i.e. the sole protected region was the hippocampus. Thus individual brain structures may have different therapeutic time windows. Selective target pathways of hypothermia remain to be determined in a region- and time-specific manner aiming at the successful development of new potential adjuvant therapies.

Even though short survival time points provide information on acute damage, brain injury can evolve for many weeks and is accompanied by endogenous regeneration processes. In agreement with Burnsed et al. we detected a loss of protection from total cerebral and cortical tissue loss (Burnsed et al., 2015). Behavioral data of the current study support the hypothesis of an endogenous recovery after HIE since Rota Rod performance improved over time in normothermic mice resulting in no net therapeutic effect compared to HT at the age of 6–7 weeks. Similarly, directed exploration of novel cues was only transiently improved. Whereas therapeutic HT did not alter undirected abnormal impulsive behavior in the Elevated Plus Maze (Ming-Yan et al., 2012; Zhu et al., 2012), HIE-induced impaired vertical activity was permanently improved by therapeutic HT independent of therapy onset. Although the detailed underlying mechanisms remain unclear, we detected a significant correlation between cortical tissue loss and rearing activity (Pearsons $r = 0.403$, $p < 0.05$) indicating that cortical circuits may be targeted by hypothermia. Nevertheless the connection between both outcome parameters was rather weak and cortical volumes were not reduced by either mode of HT application. Additional analysis of functional properties of neural cell populations and connections in specific brain regions (Belzung, 1992; Crusio, 2001; Ros-Simo and Valverde, 2012) might uncover the underlying targets of HIE-induced behavioral changes and their modulation by HT.

Despite long-term protection of the hippocampus by immediate HT, effects on functional outcome were limited which raises the question of whether cooling was too mild and/or too short. However, recent analyses in rodent and large animal models indicate that deeper and longer cooling will rather elicit harmful than beneficial effects which might be attributed to physiological responses, e.g. reduced cardiac contractility, reduced cerebral blood flow and poor perfusion (Alonso-Alconada et al., 2015; Gunn and Thoresen, 2015; Wood and Thoresen, 2015). This is supported by the clinical trial by Shankaran et al. which was stopped because the risk ratio for death during intensive care after cooling for 120 h compared to 72 h was 1.37; and in-hospital mortality rate increased from 7% to 14% when 72 h of cooling at 33.5 °C and 32 °C were compared (Shankaran et al., 2014). Thus clinical and pre-clinical data suggest that rather the onset than the depth and duration of therapy seems predictive for outcome (Gunn et al., 1998; Sabir et al., 2012). Indeed, we observed a reduction of protective capacity after a delay of 2 h in neonatal mice and further show that an endogenous compensatory down-regulation of individual body temperatures during hypoxia is highly protective.

Taken together, comparing different models of HIE and therapeutic HT in term-equivalent mice we defined a suitable model for testing adjuvant therapeutic strategies. Applying 60 min hypoxia at 10% oxygen and maintaining the nesting body core temperature followed by an immediate short and mild hypothermia closely resembles clinical conditions insofar that functional deficits are only partially improved and the therapeutic window is very short. The current study highlights that 1) body core temperatures should be kept at the physiological (i.e. nesting) level of normal uninjured subjects during hypoxia and 2) the onset of hypothermia treatment is a major determinant of therapeutic efficacy (Supplemental Fig. 8). Nevertheless, due to the limited overall efficiency, development of further adjuvant therapies is urgently needed requiring the identification of specific cellular and molecular targets of HT. According to that the use of transgenic mouse lines will be a valuable tool, provided that a well-characterized and standardized neonatal mouse model of HIE and HT is available.

Acknowledgments

This work was supported by the German Research Council (FE 518/5-1 to UFM) and by grants from the C.D. Stiftung (T228-23.816), the Karl-Heinz-Frenzen Stiftung (T328/23.433) and the Kulturstiftung, Essen. The authors thank Robert Petri for expert proofreading the manuscript as a native English scientist.

Appendix A. Supplementary data

Supplementary data to this article can be found online at http://dx.doi.org/10.1016/j.expneurol.2016.06.024.

References

Alonso-Alconada, D., Broad, K.D., Bainbridge, A., Chandrasekaran, M., Faulkner, S.D., Kerenyi, A., Hassell, J., Rocha-Ferreira, E., Hristova, M., Fleiss, B., Bennett, K., Kelen, D., Cady, E., Gressens, P., Golay, X., Robertson, N.J., 2015. Brain cell death is reduced with cooling by 3.5 degrees C to 5 degrees C but increased with cooling by 8.5 degrees C in a piglet asphyxia model. Stroke 46, 275–278.

Azzopardi, D., Strohm, B., Marlow, N., Brocklehurst, P., Deierl, A., Eddama, O., Goodwin, J., Halliday, H.L., Juszczak, E., Kapellou, O., Levene, M., Linsell, L., Omar, O., Thoresen, M., Tusor, N., Whitelaw, A., Edwards, A.D., Group, T.S., 2014. Effects of hypothermia for perinatal asphyxia on childhood outcomes. N. Engl. J. Med. 371, 140–149.

Barks, J.D., Liu, Y.Q., Shangguan, Y., Silverstein, F.S., 2010. Phenobarbital augments hypothermic neuroprotection. Pediatr. Res. 67, 532–537.

Barnett, S.A., Walker, K.Z., 1974. Early stimulation, parental behavior, and the temperature of infant mice. Dev. Psychobiol. 7, 563–577.

Belzung, C., 1992. Hippocampal mossy fibres: implication in novelty reactions or in anxiety behaviours? Behav. Brain Res. 51, 149–155.

Bevins, R.A., Besheer, J., 2006. Object recognition in rats and mice: a one-trial non-matching-to-sample learning task to study 'recognition memory'. Nat. Protoc. 1, 1306–1311.

Bona, E., Hagberg, H., Loberg, E.M., Bagenholm, R., Thoresen, M., 1998. Protective effects of moderate hypothermia after neonatal hypoxia-ischemia: short- and long-term outcome. Pediatr. Res. 43, 738–745.

Burnsed, J.C., Chavez-Valdez, R., Hossain, M.S., Kesavan, K., Martin, L.J., Zhang, J., Northington, F.J., 2015. Hypoxia-ischemia and therapeutic hypothermia in the neonatal mouse brain—a longitudinal study. PLoS One 10, e0118889.

Carlsson, Y., Wang, X., Schwendimann, L., Rousset, C.I., Jacotot, E., Gressens, P., Thoresen, M., Mallard, C., Hagberg, H., 2012. Combined effect of hypothermia and caspase-2 gene deficiency on neonatal hypoxic-ischemic brain injury. Pediatr. Res. 71, 566–572.

Crusio, W.E., 2001. Genetic dissection of mouse exploratory behaviour. Behav. Brain Res. 125, 127–132.

Dalen, M.L., Liu, X., Elstad, M., Loberg, E.M., Saugstad, O.D., Rootwelt, T., Thoresen, M., 2012. Resuscitation with 100% oxygen increases injury and counteracts the neuroprotective effect of therapeutic hypothermia in the neonatal rat. Pediatr. Res. 71, 247–252.

Ditelberg, J.S., Sheldon, R.A., Epstein, C.J., Ferriero, D.M., 1996. Brain injury after perinatal hypoxia-ischemia is exacerbated in copper/zinc superoxide dismutase transgenic mice. Pediatr. Res. 39, 204–208.

Dizon, M., Szele, F., Kessler, J.A., 2010. Hypoxia-ischemia induces an endogenous reparative response by local neural progenitors in the postnatal mouse telencephalon. Dev. Neurosci. 32, 173–183.

Griesmaier, E., Stock, K., Medek, K., Stanika, R.I., Obermair, G.J., Posod, A., Wegleiter, K., Urbanek, M., Kiechl-Kohlendorfer, U., 2014. Levetiracetam increases neonatal hypoxic-ischemic brain injury under normothermic, but not hypothermic conditions. Brain Res. 1556, 10–18.
Gunn, A.J., Thoresen, M., 2015. Animal studies of neonatal hypothermic neuroprotection have translated well in to practice. Resuscitation 97, 88–90.
Gunn, A.J., Gunn, T.R., Gunning, M.I., Williams, C.E., Gluckman, P.D., 1998. Neuroprotection with prolonged head cooling started before postischemic seizures in fetal sheep. Pediatrics 102, 1098–1106.
Hobbs, C., Thoresen, M., Tucker, A., Aquilina, K., Chakkarapani, E., Dingley, J., 2008. Xenon and hypothermia combine additively, offering long-term functional and histopathologic neuroprotection after neonatal hypoxia/ischemia. Stroke 39, 1307–1313.
Jacobs, S.E., Berg, M., Hunt, R., Tarnow-Mordi, W.O., Inder, T.E., Davis, P.G., 2013. Cooling for newborns with hypoxic ischaemic encephalopathy. Cochrane Database Syst. Rev. 1, CD003311.
Jayasinghe, D., 2015. Innate hypothermia after hypoxic ischaemic delivery. Neonatology 107, 220–223.
Kako, E., Kaneko, N., Aoyama, M., Hida, H., Takebayashi, H., Ikenaka, K., Asai, K., Togari, H., Sobue, K., Sawamoto, K., 2012. Subventricular zone-derived oligodendrogenesis in injured neonatal white matter in mice enhanced by a nonerythropoietic erythropoietin derivative. Stem Cells 30, 2234–2247.
Kida, H., Nomura, S., Shinoyama, M., Ideguchi, M., Owada, Y., Suzuki, M., 2013. The effect of hypothermia therapy on cortical laminar disruption following ischemic injury in neonatal mice. PLoS One 8, e68877.
Lin, E.P., Miles, L., Hughes, E.A., McCann, J.C., Vorhees, C.V., McAuliffe, J.J., Loepke, A.W., 2014. A combination of mild hypothermia and sevoflurane affords long-term protection in a modified neonatal mouse model of cerebral hypoxia-ischemia. Anesth. Analg. 119, 1158–1173.
Lister, R.G., 1987. The use of a plus-maze to measure anxiety in the mouse. Psychopharmacology 92, 180–185.
Liu, Y., Barks, J.D., Xu, G., Silverstein, F.S., 2004. Topiramate extends the therapeutic window for hypothermia-mediated neuroprotection after stroke in neonatal rats. Stroke 35, 1460–1465.
Liu, J., Sheldon, R.A., Segal, M.R., Kelly, M.J., Pelton, J.G., Ferriero, D.M., James, T.L., Litt, L., 2013. 1H nuclear magnetic resonance brain metabolomics in neonatal mice after hypoxia-ischemia distinguished normothermic recovery from mild hypothermia recoveries. Pediatr. Res. 74, 170–179.
Ma, D., Hossain, M., Chow, A., Arshad, M., Battson, R.M., Sanders, R.D., Mehmet, H., Edwards, A.D., Franks, N.P., Maze, M., 2005. Xenon and hypothermia combine to provide neuroprotection from neonatal asphyxia. Ann. Neurol. 58, 182–193.
Milner, L.C., Crabbe, J.C., 2008. Three murine anxiety models: results from multiple inbred strain comparisons. Genes Brain Behav. 7, 496–505.
Ming-Yan, H., Luo, Y.L., Zhang, X.C., Liu, H., Gao, R., Wu, J.J., 2012. Hypoxic-ischemic injury decreases anxiety-like behavior in rats when associated with loss of tyrosine-hydroxylase immunoreactive neurons of the substantia nigra. Braz. J. Med. Biol. Res. 45, 13–19.
Northington, F.J., Zelaya, M.E., O'Riordan, D.P., Blomgren, K., Flock, D.L., Hagberg, H., Ferriero, D.M., Martin, L.J., 2007. Failure to complete apoptosis following neonatal hypoxia-ischemia manifests as “continuum” phenotype of cell death and occurs with multiple manifestations of mitochondrial dysfunction in rodent forebrain. Neuroscience 149, 822–833.
Northington, F.J., Chavez-Valdez, R., Martin, L.J., 2011. Neuronal cell death in neonatal hypoxia-ischemia. Ann. Neurol. 69, 743–758.
Patel, S.D., Pierce, L., Ciardiello, A., Hutton, A., Paskewitz, S., Aronowitz, E., Voss, H.U., Moore, H., Vannucci, S.J., 2015. Therapeutic hypothermia and hypoxia-ischemia in the term-equivalent neonatal rat: characterization of a translational preclinical model. Pediatr. Res. 78, 264–271.
Rice 3rd, J.E., Vannucci, R.C., Brierley, J.B., 1981. The influence of immaturity on hypoxic-ischemic brain damage in the rat. Ann. Neurol. 9, 131–141.
Robertson, N.J., Nakakeeto, M., Hagmann, C., Cowan, F.M., Acolet, D., Iwata, O., Allen, E., Elbourne, D., Costello, A., Jacobs, I., 2008. Therapeutic hypothermia for birth asphyxia in low-resource settings: a pilot randomised controlled trial. Lancet 372, 801–803.
Robertson, N.J., Faulkner, S., Fleiss, B., Bainbridge, A., Andorka, C., Price, D., Powell, E., Lecky-Thompson, L., Thei, L., Chandrasekaran, M., Hristova, M., Cady, E.B., Gressens, P., Golay, X., Raivich, G., 2013. Melatonin augments hypothermic neuroprotection in a perinatal asphyxia model. Brain 136, 90–105.
Romero, J., Muniz, J., Logica Tornatore, T., Holubiec, M., Gonzalez, J., Barreto, G.E., Guelman, L., Lillig, C.H., Blanco, E., Capani, F., 2014. Dual role of astrocytes in perinatal asphyxia injury and neuroprotection. Neurosci. Lett. 565, 42–46.
Ros-Simo, C., Valverde, O., 2012. Early-life social experiences in mice affect emotional behaviour and hypothalamic–pituitary-adrenal axis function. Pharmacol. Biochem. Behav. 102, 434–441.
Sabir, H., Scull-Brown, E., Liu, X., Thoresen, M., 2012. Immediate hypothermia is not neuroprotective after severe hypoxia-ischemia and is deleterious when delayed by 12 h in neonatal rats. Stroke 43, 3364–3370.
Schlager, G.W., Griesmaier, E., Wegleiter, K., Neubauer, V., Urbanek, M., Kiechl-Kohlendorfer, U., Felderhoff-Mueser, U., Keller, M., 2011. Systemic G-CSF treatment does not improve long-term outcomes after neonatal hypoxic-ischaemic brain injury. Exp. Neurol. 230, 67–74.
Semple, B.D., Blomgren, K., Gimlin, K., Ferriero, D.M., Noble-Haeusslein, L.J., 2013. Brain development in rodents and humans: Identifying benchmarks of maturation and vulnerability to injury across species. Prog. Neurobiol. 106–107, 1–16.
Shankaran, S., Laptook, A.R., Pappas, A., McDonald, S.A., Das, A., Tyson, J.E., Poindexter, B.B., Schibler, K., Bell, E.F., Heyne, R.J., Pedroza, C., Bara, R., Van Meurs, K.P., Grisby, C., Huitema, C.M., Garg, M., Ehrenkranz, R.A., Shepherd, E.G., Chalak, L.F., Hamrick, S.E., Khan, A.M., Reynolds, A.M., Laughon, M.M., Truog, W.E., Dysart, K.C., Carlo, W.A., Walsh, M.C., Watterberg, K.L., Higgins, R.D., Eunice Kennedy Shriver National Institute of Child, H., Human Development Neonatal Research, N., 2014. Effect of depth and duration of cooling on deaths in the NICU among neonates with hypoxic ischemic encephalopathy: a randomized clinical trial. JAMA 312, 2629–2639.
Sheldon, R.A., Sedik, C., Ferriero, D.M., 1998. Strain-related brain injury in neonatal mice subjected to hypoxia-ischemia. Brain Res. 810, 114–122.
Sofroniew, M.V., 2009. Molecular dissection of reactive astrogliosis and glial scar formation. Trends Neurosci. 32, 638–647.
Thoresen, M., Bagenholm, R., Loberg, E.M., Apricena, F., Kjellmer, I., 1996. Posthypoxic cooling of neonatal rats provides protection against brain injury. Arch. Dis. Child. Fetal Neonatal Ed. 74, F3–F9.
Trescher, W.H., Ishiwa, S., Johnston, M.V., 1997. Brief post-hypoxic-ischemic hypothermia markedly delays neonatal brain injury. Brain Dev. 19, 326–338.
Villapol, S., Gelot, A., Renolleau, S., Charriaut-Marlangue, C., 2008. Astrocyte responses after neonatal ischemia: the yin and the yang. Neuroscientist 14, 339–344.
Wagner, B.P., Nedelcu, J., Martin, E., 2002. Delayed postischemic hypothermia improves long-term behavioral outcome after cerebral hypoxia-ischemia in neonatal rats. Pediatr. Res. 51, 354–360.
Walf, A.A., Frye, C.A., 2007. The use of the elevated plus maze as an assay of anxiety-related behavior in rodents. Nat. Protoc. 2, 322–328.
Wang, L., Jiang, F., Li, Q., He, X., Ma, J., 2014. Mild hypothermia combined with neural stem cell transplantation for hypoxic-ischemic encephalopathy: neuroprotective effects of combined therapy. Neural Regen. Res. 9, 1745–1752.
Wood, T., Thoresen, M., 2015. Physiological responses to hypothermia. Semin. Fetal Neonatal Med. 20, 87–96.
Xiong, M., Chen, L.X., Ma, S.M., Yang, Y., Zhou, W.H., 2013. Short-term effects of hypothermia on axonal injury, preoligodendrocyte accumulation and oligodendrocyte myelination after hypoxia-ischemia in the hippocampus of immature rat brain. Dev. Neurosci. 35, 17–27.
Yager, J.Y., Ashwal, S., 2009. Animal models of perinatal hypoxic-ischemic brain damage. Pediatr. Neurol. 40, 156–167.
Zehendner, C.M., Luhmann, H.J., Yang, J.W., 2013. A simple and novel method to monitor breathing and heart rate in awake and urethane-anesthetized newborn rodents. PLoS One 8, e62628.
Zhu, C., Wang, X., Xu, F., Qiu, L., Cheng, X., Simbruner, G., Blomgren, K., 2006. Intraischemic mild hypothermia prevents neuronal cell death and tissue loss after neonatal cerebral hypoxia-ischemia. Eur. J. Neurosci. 23, 387–393.
Zhu, W., Ma, X., Li, F., Wang, J., Yu, L., Xu, M., Ma, A., Guo, A., Zhang, N., 2012. The effect of recombinant stromal cell-derived factor-1 treatment on hypoxic-ischemic brain injury in neonatal mice. Neuropediatrics 43, 320–331.